NASA TECHNICAL NOTE

NASA TN D-6317

ELECTRON AND ION MICROPROBES APPLIED TO CHARACTERIZE AN ALUMINIDE COATING ON IN-100

by Robert M. Caves and Salvatore J. Grisaffe

Lewis Research Center
Cleveland, Ohio 44135

NATIONAL AERONAUTICS AND SPACE ADMINISTRATION • WASHINGTON, D. C. • MAY 1971

1. Report No.	2. Government Accession No.	3. Recipient's Catalog No.
NASA TN D-6317		

4. Title and Subtitle	5. Report Date
ELECTRON AND ION MICROPROBES APPLIED TO CHARACTERIZE AN ALUMINIDE COATING ON IN-100	May 1971
	6. Performing Organization Code
7. Author(s)	8. Performing Organization Report No.
Robert M. Caves and Salvatore J. Grisaffe	E-5829
	10. Work Unit No.
9. Performing Organization Name and Address	129-03
Lewis Research Center National Aeronautics and Space Administration Cleveland, Ohio 44135	11. Contract or Grant No.
	13. Type of Report and Period Covered
12. Sponsoring Agency Name and Address	Technical Note
National Aeronautics and Space Administration Washington, D.C. 20546	14. Sponsoring Agency Code

15. Supplementary Notes

16. Abstract

Exploratory analytical studies were performed on an experimental aluminide coating on the nickel alloy IN-100. The analyses included X-ray diffraction, electron beam microprobe, and an ion beam mass spectrometer probe; these analyses were supplemented by limited X-ray fluorescence and metallography. An evaluation of the analytical approaches was made with regard to their ability to characterize coatings for the high temperature oxidation protection of materials. Only qualitative information could be assigned for the approaches separately and/or collectively. Quantitative characterization of such a complex materials system was not achieved with the existing state-of-the-art analytical approaches employed.

17. Key Words (Suggested by Author(s))	18. Distribution Statement
Aluminide coating Ion beam mass spectrometer analyses Electron beam microprobe analyses Nickel-base superalloy IN-100 Oxidation protective coatings	Unclassified - unlimited

19. Security Classif. (of this report)	20. Security Classif. (of this page)	21. No. of Pages	22. Price*
Unclassified	Unclassified	32	$3.00

*For sale by the National Technical Information Service, Springfield, Virginia 22151

ELECTRON AND ION MICROPROBES APPLIED TO CHARACTERIZE AN ALUMINIDE COATING ON IN-100

by Robert M. Caves and Salvatore J. Grisaffe

Lewis Research Center

SUMMARY

An examination was made of several analytical methods to determine if, singly or in combination, they could provide a complete characterization of coating composition, coating-substrate interdiffusion, etc., for aluminide coated IN-100. X-ray diffraction, electron microprobe, and ion beam mass spectrometer probe analyses were conducted on as-coated specimens and coated specimens oxidized at 1900° F (1038° C) for 100 hours. Limited metallographic and X-ray fluorescence analyses were also performed on these materials.

No technique was able to supply a complete characterization of the coating. Even when the information from all the techniques employed was combined, it was only possible to identify the major phases present and to qualitatively establish their composition. X-ray diffraction, which is only capable of discriminating crystal structures, encountered difficulty in differentiating between phases with similar diffraction patterns and in detecting minor phases. Electron microprobe analyses provided qualitative composition data. However, difficulties in quantifying these data indicated a need for improved standards, raw data collection procedures, and computer corrections. The ion beam mass spectrometer probe (IBMS) analysis, due to the large diameter of the probe beam (approximately 300 μm), could only provide averaged results for compositional information. However, this technique required no prior specimen preparation, and it displayed a unique potential to detect all metallic and nonmetallic elements, even in trace content, throughout all coating strata. The IBMS approach would be more applicable to coating analysis if a small diameter beam were also available and if standards were improved.

INTRODUCTION

Currently, nickel- and cobalt-base superalloys for turbine engine application often are protected from high temperature oxidation/corrosion/erosion by aluminide coatings (refs. 1 and 2). These coatings are generally formed by exposing the superalloy surface to an aluminum rich environment using deposition processes such as pack cementation or slurry spraying and sintering (ref. 3). Sometimes small amounts of other elements are also intentionally (or spuriously) added to the coatings. Interdiffusion of substrate elements and coating elements during various heat treatments results in the formation of an intermetallic aluminide layer on the surface which contains some or all of the substrate and the originally introduced coating elements. This diffusion depletes the substrate of those elements that entered the coating.

During oxidation (under test or use conditions) the surface aluminide initially develops a protective aluminum oxide scale which also may contain traces of coating or substrate elements. Further exposure produces a mixed oxide scale containing aluminum oxide and complex spinels. Thus, even "simple" aluminide coatings can involve one or more oxides, an intermetallic layer(s), a diffusion affected zone(s), and the base metal substrate. Each of these consists of a number of major and minor phases, and each contains many elements which can, in an as yet unknown way, influence the thermal, physical, and protective nature of the coating.

Knowledge of the distribution of major elements is, of course, important to the understanding and performance improvement of aluminide coatings. However, minor quantities of certain elements can also exert a major effect on oxidation resistance of intermetallics and alloys. For example, as little as 0.5 percent yttrium substantially improves the oxidation resistance of iron-chromium (Fe-Cr) alloys (ref. 4). Since most commercial aluminide coatings are proprietary, little information has been presented on their composition. Where coating analysis studies have been conducted (refs. 1 to 3), emphasis has usually been placed on selected major elements only.

This report contains the results of a program conducted at the Lewis Research Center to examine several available analytical approaches to determine if singly or in combination they could characterize all phases of a multicomponent aluminide coating. This examination was made from the viewpoint of one who must obtain data from several analytical methods and integrate the information into a rational interpretation of composition effects on coating performance.

Here an experimental aluminide coating and the underlying nickel-base superalloy substrate IN-100 were analyzed in the as-coated condition and after 100 hours of cyclic air oxidation at 1900^{o} F (1038^{o} C). X-ray diffraction (XRD), electron microprobe (EMP), and ion beam mass spectrometer probe (IBMS) analyses were the primary

analytical techniques. The uncoated IN-100 substrate was also analyzed by chemical analysis. Limited use was made of metallography and X-ray fluorescence (XRF) to supplement these analytical techniques.

EXPERIMENTAL

Materials

The nickel-base superalloy IN-100 was used as the substrate material in this study. It was commercially produced by casting in the form of plates, approximately 2 by 1 by 0.1 inch (5 by 2.5 by 0.25 cm) thick, and in the form of bars, approximately 4 by 1 by 1/4 inch (10 by 2.5 by 0.6 cm) thick, to the same chemical specifications. Since the bulk of the analytical work was conducted on plate specimens, both vendor and independent laboratory analyses of the plate material are presented in table I. Both sets of data show good agreement, but because of the completeness of the independent laboratory analysis, this analysis will be used as a reference for comparison with analyses by the other analytical procedures.

All uncoated specimens for EMP and IBMS analyses were cut from a single flat plate casting and were approximately 7/16 by 7/16 by 0.1 inch (1 by 1 by 0.2 cm). Some cast bars were sectioned into specimens approximately 1 by 0.25 by 0.1 inch (2.5 by 0.6 by 0.25 cm). All specimens were then coated in a single batch by the coating vendor. Similar small analytical specimens were cut from these as well. Specimens for qualitative XRD analyses of the coating phases were obtained from segments of cast bars only, since metallographic analyses showed that the proprietary coating was essentially identical on both plate and bar specimens. No details of the coating process (or processes) or of the coating composition were supplied by the vendor other than an indication that this was an experimental chromium-aluminide coating applied in a single batch.

Some coated specimens, supported on pure alumina boats, were oxidized in slowly flowing air (2 SCFH or 0.5 liter/min) at 1900^{o} F (1038^{o} C) for a total of 100 hours using 20-hour thermal cycles. (A cycle was 20 hours at the high temperature followed by rapid cooling to room temperature and reheating.) Both as-coated and as-coated/oxidized specimens were sent out for vendor ion beam mass spectrometric (IBMS) analysis. This analysis can be performed on unprepared surfaces of unmounted specimens. Concurrent with the IBMS analysis, companion specimens from the coating batch were metallographically mounted, sectioned, polished, and etched. The desired path for electron microprobe analysis was marked by Knoop hardness indentations using a 500-gram load. After a very light diamond polish to remove the etched surface, these specimens were then sent out for vendor electron microprobe analyses. Other similarly coated and oxidized bar specimens were submitted for qualitative XRD analysis.

TABLE I. - ANALYSIS OF IN-100 (HEAT RU-188)

IN THE AS-CAST CONDITION BEFORE COATING

[Analyzed by standard wet chemistry and spectrochemical methods.]

Elements	Vendor analysis, wt %	NASA reference chemical analysis,[a] wt %
Major metallic		
Al	5.59	5.33
Co	15.15	15.37
Cr	9.70	9.50
Mo	3.20	3.17
Ni	60.62[b]	61.14
Ti	4.34	4.26
V	.92	.82
Minor metallic		
B	0.011	0.0199
Ca	-----	.003
Ce	-----	.0005
Cu	-----	.05
Fe	.11	.20
Mg	.00	.001
Mn	.1	.003
Nb	-----	.10
Si	.1	.08
Ta	-----	.05
W	-----	.05
Y	-----	.0005
Zn	-----	.03
Zr	.06	.087
Nonmetallic		
C	0.17	0.166
H	-----	.00013
Halogens:[c]		
F	-----	(c)
Cl	-----	(c)
Br	-----	(c)
I	-----	(c)
N	-----	.0060
O	-----	.0119
P	-----	.0110
S	.003	.0080
	Total 100.	Total 100.46

[a]Analysis performed by independent analytical laboratory and is used as the reference analysis for comparison purposes.

[b]Value for Ni obtained by difference of other elements from 100 percent.

[c]No established analytical method is available for use with Ni or Co base superalloys.

Analysis

Electron microprobe. - The basic method of analysis for the electron microprobe is schematically presented in figure 1(a). In the electron microprobe, a 1-micrometer (micron)-diameter beam of primary electrons is used to bombard a small target area to excite the emission of characteristic X-rays from a hemisphere approximately 3 micrometers in diameter. The wavelengths and intensities of these X-rays can be interpreted to give qualitative information on the elements present in the target area, much as with X-ray fluorescence.

Analyses were conducted independently by two EMP contractors, each used the same basic make and model instrument. Contractor A conducted the bulk of the reported analyses, while contractor B performed raster scans and some cross-checking of selected elements. A more detailed description of their analytical procedures is presented in appendix A. Both contractors traversed the same analytical path within the limits optically discernible by the carbonaceous tracks left after analysis. Both used elemental standards for all of the elements except that pure aluminum oxide was used as a standard for aluminum and oxygen in the oxide phase. Because of the presence of so many phases, and the fact that no matrix standards were available for each, the intensity data were only converted to approximate weight percentages by using the ratio between the measured intensity in the analysis and that from the elemental standard. No corrections for absorption, fluorescence, or atomic number were made because computer programs now available will not normally accommodate the total number of elements encountered in such coated superalloy systems.

Ion beam mass spectrometer probe. - The ion beam mass spectrometer probe is a relatively new macro- or semi-micro-analytical instrument which is still under development (refs. 5 to 9). Figure 1(b) is a simplified schematic representation of a specimen undergoing analysis with the ion beam mass spectrometer probe. Here no prior specimen surface preparation is required. A focused energetic primary beam of argon ions, approximately 300 micrometers in diameter, impinges on the specimen surface and bores (sputter-erodes) a hole in it. The constituents are ionized and these secondary ions emanate from the eroded surface and enter a mass spectrometer. The analyses were performed with a mass spectrometer that was both double focusing and stigmatic imaging, and the details for such analyses are presented in appendix B. Because of the type spectrometer employed, the mass-to-charge resolution and sensitivity were claimed by the contractor to be quite high - the latter reportedly can be in the parts per billion range. However, for the purpose of this study, analytical limits only above 10 parts per million (ppm) were used. Full spectral scans and measurements for ion species with mass-to-charge ratios from 1 to 1000 can be made with this device. Thus, all isotopes of elements

throughout the periodic table may be analyzed except in cases where species have overlapping spectral peaks.

Preliminary analyses at the surface of the specimens used in this study showed no appreciable concentration of species with mass-to-charge ratios above 200. This was then selected as the cutoff value for analysis.

The resulting intensity-time data for prominent mass-to-charge species less than 200 to 1 were converted to concentration-depth data by the use of contractor developed intensity yield factors. The yield factors, assumed to be constant with coating depth, were obtained from substitute standards (appendix B) and from measured rates of surface penetration.

X-ray analysis. - Standard powder X-ray diffraction procedures were employed on samples of as-coated and as-coated/oxidized bar specimens to provide some qualitative insight into the phases present in each condition. Powder samples were removed from the surfaces by a series of successive hand filing operations until major substrate phases were detected. Due to the wide variety in layer hardness, it was not possible to remove uniformly thick layers for these analyses. Therefore, the phases cannot be directly related to depth in cross-sectional microstructures but can only be indirectly correlated with microprobe and ion probe results.

RESULTS AND DISCUSSION

General Nature of the Coating

Unetched photomicrographs of the coated specimen cross section in the as-deposited coating condition and a similar cross section of the coating after oxidation are shown in figure 2. As will be established later, the as-deposited coating (fig. 2(a)) was essentially an iron-nickel aluminide. Large aluminum oxide particles (dark gray) are trapped in the surface (presumably from a pack cementation process), while finer aluminum oxide particles (dark gray) were found near what appears to have been the original coating-substrate interface. These may have been added to serve as a partial diffusion barrier. This region also appears to contain MC (M for metal) carbide particles (refs. 1 and 2). There was no gamma prime (M_3Al) layer detected beneath the coating as is sometimes found in aluminide coatings (ref. 3), but rather there is a solid solution zone depleted in nickel.

The as-coated/oxidized specimen (fig. 2(b)) shows a thin white M_3Al layer, still rich in iron, directly beneath the large gray alumina particles and the lighter gray mixed oxide surface scale that formed on oxidation exposure. The M_3Al layer developed near the coating surface due to aluminum depletion of MAl which occurs as the alumina surface oxide scale forms and then spalls on thermal cycling. Also, this figure shows that there

was an increase in the carbide phase particles in the region containing the internal small gray aluminum oxide grains. These carbides appeared to extend into the unaffected substrate. Iron diffusion from the coating into the substrate apparently destabilized the gamma/gamma prime microstructure of the IN-100 to the extent as indicated in figure 2(b). This zone was very hard.

X-Ray Diffraction

The qualitative X-ray diffraction results for progressive, depth-wise samples (depth not measured) are presented in table II for the as-coated condition and in table III for the coated/oxidized condition. As indicated in table II, very strong intensity MAl (or solid solution alpha iron or chromium) and alumina (large crystals) diffraction patterns were observed near the coating surface. Since the MAl phase and alpha iron or chromium phases have essentially the same diffraction patterns and lattice parameters, they can only be differentiated in XRD by the presence of a few weak lines. When these lines are

TABLE II. - PHASES DETECTED BY X-RAY DIFFRACTION AT SUCCESSIVE DEPTHS

INWARD FROM THE SURFACE OF ALUMINIDE COATED IN-100

Arbitrary sample depth location	Intensity of detected phases		
	Strong	Medium	Weak
1	α Al_2O_3[a] (large crystals) MAl (or α Fe, Cr)[a]	----------	----------
2	α Al_2O_3 (large crystals) MAl	----------	----------
3	α Al_2O_3 (large crystals) MAl	----------	----------
4	α Al_2O_3 (smaller crystals) MAl[a]	----------	----------
5	MAl[a]	α Al_2O_3 (small crystals)	----------
6	MAl[a]	----------	α Al_2O_3 (small crystals)
7	MAl	α Al_2O_3 (small crystals)	----------
8	MAl[a]	----------	α Al_2O_3
9	MAl[a] Ni solid solution[a]	----------	TiO or NiO
10, 11, 12	Ni solid solution	MAl	α Al_2O_3[b]
13	Ni solid solution[c]	----------	MAl or α Fe, Cr

[a]Intensity, very strong.
[b]Intensity, very very weak.
[c]Believed to be IN-100.

TABLE III. - PHASES PRESENT AT SUCCESSIVE DEPTHS

IN AN OXIDIZED, ALUMINIDE COATING ON IN-100

Arbitrary sample depth location	Intensity of detected phases		
	Strong	Medium	Weak
1	M_3Al[a] α Al_2O_3 (large crystals)	Fe_4Al_{13}	MAl
2	M_3Al α Al_2O_3 (large crystals)	-------	MAl Cr_3Al_2
3	α Al_2O_3 (small crystals) M_3Al	-------	MAl
4	α Al_2O_3 MAl	-------	------
5	α Al_2O_3	MAl	------
6	α Al_2O_3 MAl	-------	------
7	α Al_2O_3 MAl	-------	------
8, 9, 10, 11, 12	MAl	α Al_2O_3	------
13	MAl[a] (XRF: Ni, Fe, Cr, Co, Mo)	α Al_2O_3	------
14	Ni solid solution (XRF: Ni, Cr, Co, Mo) M_3Al	-------	------

[a]Intensity, very strong.

weak or missing as frequently occurs (see appendix C), X-ray diffraction cannot differentiate between MAl and alpha iron or chromium. Since the coating was rich in aluminum, as determined by EMP, the major phase was determined to be MAl. Deeper in the coating a fine grained alumina was detected with the MAl phase. At still greater depths, the nickel solid solution (gamma) phase was detected. The intensity of the MAl phase decreased in samples as penetration to greater depths was made toward the solid solution zone.

The oxidized coating (table III) shows the presence of M_3Al, alumina (Al_2O_3), and, to a lesser extent, MAl near the surface. Also present were Fe_4Al_{13} and Cr_3Al_2. Neither of the latter phases was detected in the as-coated specimen but could have been present in amounts near, but below, the detectability limits of XRD - usually 1 to 5 percent. At greater depths, the phases observed were similar to those in the as-coated specimen - namely, MAl, fine grained alumina, gamma solid solution, and, in addition, gamma prime (M_3Al). At depths where no MAl or alumina were detected, the nickel

solid solution no longer showed any iron under X-ray fluorescence analysis.

In all of these cases, phases were identified by first measuring all of the interplaner spacings produced when the powder samples were subjected to diffraction. By comparison with reported data (ref. 10), these lattice spacings were then ascribed to individual phases. However, as previously pointed out, there are many cases where diffraction patterns overlap or the spacings do not agree with the reported data from high purity, single phase materials. These limitations, together with the requirement for between 1 and 5 percent of a phase to be present before it is detected by routine XRD, create uncertainties in the analytical results that are seldom reflected in the literature. Since X-ray diffraction can only identify crystal structures, and not phase chemistry, adjunctive techniques such as EMP are also commonly used in analyzing coatings.

Electron Microprobe Analysis

Electron microprobe data were obtained on cross sections of cast IN-100, as-coated IN-100, and coated/oxidized IN-100. In this report the ratios of the electron microprobe apparent net intensity data (see appendix A) to the net intensity of pure elemental standards provide a first approximation of element concentrations in weight percent. For some major elements in the as-cast IN-100, these data are in fair agreement with the reference chemical analysis as shown in figure 3 (e.g., Ni measured about 52 percent as compared to 61 percent in the reference analysis). Figure 3 also includes a micrograph of an etched cross section of uncoated IN-100 with the microprobe path sketched in as a dashed line. The corresponding EMP concentration profiles as functions of depth from the surface are presented below the photomicrograph using the same vertical scale in all three plots. This figure also presents the reference chemical analysis from table I for the same nine major elements in the alloy included in the concentration profiles.

The microstructure in figure 3 contains a salt and pepper mixture of white gamma prime and gray gamma-solid solution of nickel, cobalt, chromium, etc. The massive white areas are primary gamma prime, but they also generally contain some MC and $M_{23}C_6$ carbides. The uncorrected EMP data show the nickel in the substrate to be around 50 percent. This is lower than the 61 percent determined by the reference chemical analysis. According to the EMP data, the cobalt is around 16 percent and is not far from the reference analysis value of 15 percent. Chromium is somewhat higher than the reference analysis (12 percent against 9.5 percent), while most of the other elements are low. Aluminum is especially depressed at 2 percent instead of 5.3 percent. This is caused by the high mass absorption coefficient of nickel for the K-alpha radiation of aluminum. Note that the peaks for molybdenum, titanium, chromium, and carbon frequently coincide except where prominent areas of the primary gamma prime are encoun-

tered. For example, at a depth of between 125 and 150 micrometers (5 and 6 mils), these peaks probably suggest the presence of MC and/or $M_{23}C_6$ carbides which are known to exist in IN-100 (ref. 11).

The concentration data (first approximation) for the as-coated specimen are presented in figure 4. In addition, this figure contains raster scanning micrographs at the right. The dark field in the backscatter electron (BSE) micrograph represents low average atomic number regions. In the cathode luminescence (C-L) micrograph the bright areas mirror image a low atomic number oxide as being present at the surface of the specimen and at a depth of about 100 micrometers (4 mils). (The BSE is dark in these areas, whereas the C-L is white.) In addition, a high atomic number region at 100 to 150 micrometers (4 to 6 mils) depth is indicated. Later this was proved to be an artifact, identified as Th, possibly introduced during metallographic preparation. The scans for aluminum and iron show high concentrations in the coating while chromium, except for scattered spots to 100 micrometers (4 mils) in depth in the coating, appears uniformly distributed in the substrate. The concentration-depth data are shown below the optical photomicrograph of the coating (left) substrate (right) cross section. The use of alumina as a primary standard seemed to provide concentration values for aluminum closely approximate to the phases known to be present. (For the convenience of the reader, the optical micrograph has been marked with zone numbers to designate the principal strata.)

In zone I, the high aluminum and oxygen peaks and the absence of any other elements confirms the XRD findings of aluminum oxide. The aluminum peak is high - 65 percent instead of the stoichiometric 53 percent - while the oxygen peak (47 percent) coincides with the known oxygen level in alumina. The agreement should be good here, since aluminum oxide was used as the standard for both these elements. Some of the difference in the aluminum values may be due to uncertainties in the microprobe analyses.

In zone II, the aluminum level was about 34 percent. Cobalt and nickel both showed increasing concentrations across this zone. Cobalt increased from 2 to 13 percent and nickel from 2 to 30 percent. Iron, however, was observed to decrease from 42 to 18 percent. These values reasonably approximate the composition of MAl (β aluminide) with a varying composition of iron, cobalt, or nickel.

Zone III shows high aluminum, titanium, and chromium levels with peaks for oxygen, molybdenum, and carbon. The nickel, cobalt, and iron levels decrease in this zone. Combining this information with the XRD data, the small gray particles were identified as aluminum oxide. The lack of apparent stoichiometry (i.e., the low detected oxygen level) is attributed to the very small oxide particles (less than 1 micron diameter). The microprobe beam is not able to resolve the analysis of particles that small and the results are an average of the well dispersed particles and surrounding aluminum-rich matrix. MC carbides (refs. 1 and 2) in IN-100 are primarily of the (Ti, Mo) C type. The chromium peak may be related to particles of a chromium rich carbide and/or particles of a chromium aluminide.

Zone IV may contain a few carbides, but generally it appears to be a solid solution region rich in iron and lower in nickel and cobalt than the IN-100 substrate. Note again, that the carbide particle intersected at a depth of 200+ micrometers (8+ mils)(zone V) is rich in titanium and molybdenum.

Figure 5 contains concentration data (first approximation) for aluminum, oxygen, chromium, nickel, cobalt, iron, carbon, molybdenum, titanium, and vanadium in the oxidized coating specimen.

The optical photomicrograph at the top of figure 5 shows that several microstructural changes have occurred in the coating during the 100 hour at 1900° F (1038° C) oxidation exposure. These observations are confirmed by the probe data presented below the photomicrograph.

In zone I (fig. 5), in addition to the Al_2O_3 observed in figure 4, peaks for chromium, nickel, and carbon can also be seen. While the aluminum peak is again high, 66 percent instead of 53 percent, the oxygen peak is in agreement with the oxygen content of Al_2O_3 (47 percent). The chromium may be present in several forms. It could be in solid solution with Al_2O_3 or present as small amounts of Cr_2O_3 - an oxide isomorphous with alumina - or as a chromium rich aluminide or a carbide phase not detected by XRD. The nickel is probably present as a $NiAl_2O_4$ spinel, but again, the amount of that oxide present must have been so low as to escape detection by XRD. Such a spinel is sometimes found in the oxide scale formed on a nickel aluminide coating after prolonged high temperature oxidation exposure.

Zone II generally shows a low aluminum concentration (approximately 5 percent) with an aluminum peak coinciding with the very high iron peak. In zone III, which is primarily MAl, the aluminum concentration is again depressed. This depression (not seen in fig. 4) can, in part, be traced to the mass absorption coefficient of nickel that has diffused into the coating. This coefficient is about 25 to 30 percent higher than that of iron for long wavelength radiation such as the K alpha of aluminum (8.33 Å). Thus, the iron rich as-deposited coating would absorb less aluminum radiation and appear to have a higher aluminum content than the nickel rich exposed coating. Also, part of this decrease in aluminum can be attributed to inward diffusion. After 100 hours, the aluminum concentration has leveled off at a depth of 200 micrometers (8 mils) rather than at 125 micrometers (5 mils) in the as-coated specimen (fig. 4). The aluminum peaks again appear associated with the gray oxide particles. The sum of the cobalt, iron, and nickel levels approximates that expected in an MAl phase. Zone III also contains more white, blocky particles which are believed to be MC carbides. These carbides have the same appearance in the coating as in the IN-100. In some places where the probe track passed over these particles, titanium peaks, but no carbon peaks, were detected.

Zone IV shows aluminum and oxygen peaks - both depressed from the values for Al_2O_3 and similar to those observed in figure 4. This region of depressed iron, cobalt,

and nickel has peaks for chromium, titanium, molybdenum, vanadium, and carbon indicating the presence of carbides - most likely of the MC type but with the possibility of also containing some $M_{23}C_6$. Zone V shows the development of distinctive particles (grains) in contrast to the structure as the similar zone (IV) for the as-coated material in figure 4. Again peaks for chromium, molybdenum, titanium, vanadium, and carbon are present suggesting carbides similar to those observed in zone IV. Zone VI is similar to zones IV and V but the aluminum content is lower. From the composition data, this zone still appears to be a solid solution zone - no M_3Al was detected by XRD. Since it etches more like M_3Al, it might be an aluminum rich solid solution zone. Zone VII is the substrate.

While many of the approximate concentrations of the transition metals (Ni, Co, Fe, and Cr) established previously showed reasonable agreement with the reference chemical analysis or with known phase compositions, other elemental concentrations differed markedly. Some of these differences can be traced to the data correction procedure used in this report for no computer corrections were made for matrix, mass absorption, fluorescence, atomic number, instrument variables, etc. However, in considering computer corrections and their applicability to the data of this report, it is interesting to examine table IV (ref. 12). Here different computer programs and mass absorption coefficient corrections (MAC) were used in an attempt to correct raw EMP data so as to quantitatively establish the composition of pure, single phase matrices of Ni_3Al, NiAl, and several carbides which had also been analyzed chemically. Note, for example, that the corrected aluminum content of NiAl (34.4 percent Al) varied from 27 to 52 percent. Thus, the current corrective procedures leave much to be desired for quantitative accuracy, even for binary, bulk phases. Less accuracy is possible when many phases of varying stoichiometry are present.

As shown in appendix C, phases of the type traversed in the present program can be much more chemically complex than the single, binary phases in table IV. Also, individual particles of varying thickness allow varying contributions from the materials beneath the surface to further affect the accuracy of EMP analysis. Finally, the EMP has low sensitivity to low atomic number elements and can fail altogether to detect trace elements. These factors all contribute to a level of uncertainty rarely reflected in the literature. For this reason further analytical efforts on coatings could benefit from improved data acquisition and correction factors, development of better standards, and increased instrument sensitivity.

TABLE IV. - COMPARISON BETWEEN CHEMICAL AND ELECTRON MICROPROBE ANALYSES FOR PURE SINGLE PHASE MATERIALS COMMONLY FOUND IN ALUMINIDE COATED NICKEL ALLOYS (REF. 12)

	Single phase materials							
	Ni_3Al		NiAl		Equiaxed nickel alloy carbide			
	Ni	Al	Ni	Al	Cr	Co	Ni	W
Nominal composition of bulk material, percent	13.3	86.7	34.4	65.6	(a)	(a)	(a)	(a)
Electron probe microanalysis, measured raw concentration, percent	2.5	87.8	8.9	64.7	26.6	2.3	23.6	33.3
Standard program corrected concentration at 5th iteration:								
Heinrich's MAC[b]	8.8	88.2	27.3	67	28.2	3.5	21.4	42.4
Birks' MAC[b]	12.7	88.2	37.0	67.9	28.5	3.5	21.3	41.9
'Raw' program corrected concentration at 5th iteration:								
Heinrich's MAC[b]	8.3	87.9	24.6	66.3	27.6	3.4	21.0	41.8
Birks' MAC[b]	13.1	89.0	40.9	68.6	28.0	3.5	20.9	41.4
Normalized program corrected concentration at 5th iteration:								
Heinrich's MAC[b]	9.9	99.4	38.4	94.2	34.3	4.3	26.0	51.6
Birks' MAC[b]	14.3	100	52.1	95.4	34.7	4.3	25.9	51.0

[a]Not determined.

[b]Mass absorbtion coefficient, MAC.

IBMS ANALYSIS

The results for the contractor analysis of the uncoated IN-100 are shown in table V, while those for the coated IN-100 are presented in figures 6 (as-coated) and 7 (coated and oxidized). Since a large crater of the material is removed by ion bombardment in this analysis, no microstructures of the exact sections analyzed can be presented. However, the specimens analyzed by this technique were companions to the coated plates analyzed by EMP. Because the reproducibility of the coatings was judged good

TABLE V. - COMPARISON OF IBMS ANALYSIS OF SUBSTRATE WITHIN AS-COATED SPECIMEN TO A DEPTH OF 225 TO 250 μm (9 TO 10 MIL) WITH REFERENCE CHEMICAL ANALYSIS (TABLE I) OF UNCOATED IN-100

Elements	Concentration, wt %	
	Reference chemical analysis	IBMS analysis
Major constituents		
Ni	61.14	59
Co	15.37	10
Cr	9.50	6.5
Al	5.33	5.5
Ti	4.26	5.5
Mo	3.17	1
Minor constituents		
V	0.82	6
Fe	.20	7
C	.166	.5
O	.0119	.5
N	.0060	.07

based on microstructural examination, typical photomicrographs to the approximate scale as the graphs are presented at the tops of figures 6 and 7 for reference. Since the IBMS was able to detect much wider concentration ranges of elements than the EMP, the data in figures 6 and 7 are presented as log concentration against depth in contrast to the linear scales used in figures 4 and 5. Because a much larger area was analyzed than in EMP analysis, the averaged concentrations changed much more gradually than the changes measured by EMP.

The IBMS detected and analyzed for nickel, iron, cobalt, chromium, aluminum, titanium, vanadium, molybdenum, oxygen, and carbon just as was generally done in EMP analysis. The prominent iron concentration in the coating was first revealed in the IBMS analysis. Iron could have been detected by XRF or EMP, but it probably would

not have been as the normal procedures do not include spectral scans in each strata. In addition, IBMS analysis detected the presence of nitrogen and fluorine. The concentration data for all these elements are presented in figures 6 and 7.

Table V compares the IBMS data (corrected to a first approximation of weight percentages) with the reference chemical analysis. The results are considered reasonable for this relatively new technique, especially for the major elements which comprise 98 percent of the substrate. For example, nickel was determined to be 59 percent by IBMS, while chemical analysis indicated it to be 61 percent. Only vanadium, iron, oxygen, molybdenum, and nitrogen data differ significantly from the chemically analyzed IN-100 composition. For example, the chemical analysis indicated that 3 percent molybdenum was present, while the IBMS analysis indicated only about 1 percent. These errors are believed to be due to low accuracy intensity yield factors used to convert the raw data since these elements are more or less uniformly distributed throughout the substrate.

In figure 6 the concentration trends of nickel, cobalt, chromium, aluminum, oxygen, iron, etc. are similar to those determined by EMP. Aluminum and oxygen peaks near the surface and at a depth of 100 to 125 micrometers (4 to 5 mils) again reflect the presence of Al_2O_3. Iron shows a high concentration in the coating and then drops off to the alloy background level value at approximately 125 micrometers (5 mils). The other elements are generally lower in the coating and increase in the substrate. In the 75 to 150 micrometers (3 to 6 mil) depth range, carbon, fluorine, and nitrogen concentrations were observed. As nitrogen could be prominent in the high temperature environments and also readily associates with carbides, the presence of carbon and nitrogen near the coating surface in trace quantities is not altogether a surprise. However, fluorine was not expected to be present. The concentration of fluorine may well be due to the use of a fluoride activator in the pack cementation coating processes used to deposit this complex aluminide coating. Some, if not all, of the nitrogen, as well as the fluorine, could have been added if the activator were of the ammonium fluoride type.

In figure 7, for the coated/oxidized specimen analyzed by IBMS, the same general changes in concentration against depth observed in EMP analysis were again observed. Vanadium, titanium, molybdenum, chromium, carbon, and nitrogen all show increased concentration in the 125 to 250 micrometers (5 to 10 mil) depth range - the same zone visually seen to be enriched in carbides. Also note that the fluorine appears to have diffused inward for it now peaks (~ 0.3 percent) near a 125-micrometer (5-mil) depth instead of at the 75-micrometer (3-mil) depth shown in figure 6.

Although the effects of residual activator elements are unknown, they could play an important role in coating oxidation mechanisms. The IBMS, then, provides the first readily available analytical approach for routinely detecting trace or major quantities of metals or nonmetals, and with a minimum amount of damage to a superalloy specimen.

However, a reduction in the primary beam size is needed to achieve microstructural analysis with this instrument. Also, the accuracy of the intensity yield factors ultimately must be improved. If such improvements can be made, this approach would offer a very sensitive device with wide range for analytical capability. A prime advantage of this instrument, even at its present early stage of development, is the ability to simultaneously analyze for all elements.

CONCLUDING REMARKS

An exploratory effort was made to determine if several analytical techniques, singly or in combination, could characterize the phases present in an aluminide coated IN-100 superalloy. This effort was primarily made from the viewpoint of an investigator who must gain understanding of coating compositions before he can rationally develop improved protection systems. X-ray diffraction, electron microprobe, ion beam mass spectrometer probe, X-ray fluorescence, and metallography were used to examine an experimental aluminide coating before and after oxidation for 100 hours at 1900° F (20-hr cycles). For base line information, the uncoated alloy was examined.

From this study it was possible to combine the information from the various analytical techniques and determine that the as-deposited coating contained surface particles of aluminum oxide which were entrapped in an iron-rich MAl layer. The MAl contained interdispersed titanium, molybdenum rich carbides, and small aluminum oxide particles. Beneath this primary protective layer an aluminum-rich nickel depleted solid solution region was observed. After oxidation exposure, surface depletion of aluminum produced some M_3Al and additional carbides in the solid solution zone beneath the coating. The exact composition of the phases present was not established by these analyses, however.

In general, no one analytical technique provided enough information to characterize the coating or substrate phases. Even when information from all of the analytical techniques was combined, it was possible to develop only a qualitative understanding of the phases present and their compositions.

As a result of this study, some insights were gained into the applicability of the analytical procedures employed for use in coating characterization. These are now summarized.

1. X-ray diffraction is the only approach able to establish the crystal structure of the individual phases. It can identify such phases if they are present in concentrations above 1 to 5 percent. Many of the phases present in aluminide coatings on nickel superalloys, however, have overlapping or nearly identical diffraction patterns. In some of these cases, supplemental EMP or metallography must be used to even determine which phase is really present. EMP or some other technique is also required to introduce

compositional information into an analysis, for X-ray diffraction cannot provide such information.

2. The electron beam microprobe is a good qualitative microanalytical tool (1 to 3 micrometer area analyzed) and both raster scans and element traces can provide considerable insight into the composition of minor phases and into the composition gradients that exist in aluminide coatings. Spectral scans should be conducted in representative areas of the coating and substrate so as to establish those elements present for subsequent microprobe analysis. In some instances in this study the first approximation of actual weight percentages from element traces did not differ greatly from chemical analysis data. However, the raw or corrected EMP data do not appear to quantitatively reflect small changes in phase composition which must occur during coating exposure. The EMP data resulting from the analysis of such complex systems must be viewed only as qualitative until accurate standards of similar composition to each coating phase can be established and until specimen current and signal-to-background ratios (appendix A) are routinely monitored. Such changes in these values will also be required for corrections for mass absorption coefficient, atomic number, etc., and until such computer corrections can be extended to handle the many elements normally present in complex aluminide coated superalloys.

3. The ion beam mass spectrometer (IBMS) has the ability to qualitatively scan coatings and detect the presence of unexpected, spurious, and/or trace quantities (ppm range) of both metallic and nonmetallic elements. Presently the IBMS is only a semi-micro tool since it has a beam diameter of approximately 300 microns (100 times larger than EMP). Thus, the resulting composition data represent an average of the many phases being probed at one time. While with some systems this may even be an advantage, it makes small compositional changes in any one phase almost impossible to follow. As with the EMP, better standards and correction procedures appear necessary if anything other than qualitative analyses are to be obtained. A smaller beam diameter would greatly extend the usefulness of this type of instrument.

Lewis Research Center,
National Aeronautics and Space Administration,
Cleveland, Ohio, January 21, 1971,
129-03.

APPENDIX A

ELECTRON MICROPROBE CONSIDERATIONS

Both contractors A and B used 2-micrometer interval step scans over a path marked with microhardness indentations. Specimen current and signal-to-background ratios were not routinely monitored across each strata of the complex system by either contractor. This monitoring entails extra effort on the part of the operator and, of course, additional expense. But valid data either for qualitative interpretation or for computer correction procedures are not produced if such monitoring is overlooked. This operational procedure can be as significant to the results obtained as the use of the elemental standards. Yet lack of indication whether or not the monitoring was performed often is a serious omission from much of the literature reporting EMP analyses.

Contractor A analyzed the specimens for nine preselected elements. The selection was based on the uncoated substrate reference chemical analysis described in table I and on anticipated constituents in the coating. Unfortunately, spectral scan analysis for all other possible elements was not requested from this contractor. However, future efforts would benefit from such scans.

The accelerating potential used by contractor A was 20 kilovolts. In addition, the standards adopted for calibration were the corresponding pure elements except for oxygen. Here pure aluminum oxide was used. Three different elements were measured through the dispersive X-ray channels during each traverse, and accumulated counts were taken for 30 seconds at each step. Successive traverses with a new set of three elements each time were continued until the intensities of all nine preselected elements were determined.

Contractor B chose to use 30 kilovolts for the accelerating potential. The counting period used at the step positions was only 5 seconds in these analyses. The same beam path was followed as that used by contractor A (within the limits of postanalysis optical discernibility). Contractor B experienced some beam wander near the edge of the specimens but eliminated this problem by application of an evaporative conductive coating of carbon on the specimen surface. This and normal pump oil cracking, of course, increased the carbon background level. Contractor B initially used the reference chemical analysis of the substrate alloy as the standard in calibration of aluminum, chromium, nickel, and vanadium. The standard used for iron was the pure element. These data appeared slightly less accurate than when pure standards were used but since only five elements were analyzed, this distinction is not straightforward. In all cases, the aluminum data from contractor B were depressed with respect to known values for alumina and the aluminide coating and more closely agree with the uncorrected EMP data presented in table IV for bulk NiAl.

In contractor B's analyses, aluminum was measured through one spectrometer for each traverse while each two of the remaining elements were being measured. The resulting duplicate concentration-depth profiles of aluminum were intended as a reference to ensure that lineal registry could be obtained for all other element profiles, particularly if micrometer measurement or beam wander were not properly controlled. In addition, the repetitive profiles obtained for aluminum served to establish how well the contractor was able to retrace a desired analytical path.

It is noteworthy that the contractor B analyst, after completing the initial analyses for five elements, voluntarily quoted "confidence in the accuracy" for aluminum, chromium, nickel, and vanadium in the alloy substrate as being ±1 percent; for iron in the coating as being within ±5 percent; and a confidence in the accuracy for all elements in the coating area, conservatively, as being within ±10 percent. The aluminum concentration alone is off by more than 70 percent. Obviously, precision and accuracy are often misapplied, even by some analysts. Upon reanalysis of the oxidized specimen for all detectable elements, the analyst found that special calibration curves were necessary for molybdenum and titanium because the background levels for the former were unusually high while those for the latter were depressed.

APPENDIX B

ION BEAM MASS SPECTROMETER CONSIDERATIONS

In the ion beam mass spectrometer analytical process, the spectral intensity peaks for the constituent element ions were obtained using an energy window of 250 electron-volts. Use of this energy window reduces the interference of molecular spectra and element spectra are thereby more clearly separated and measured.

The analyses were performed at 15-micrometer step intervals from the surface, without interruption of sputter boring. During each analysis the beam penetrated from 1 to 2.6 micrometers in 1 to 2 minutes. These were sufficient times for the magnetic field to be swept by hand from peak to peak, and for sufficient holds at the peaks for integrated counts of intensity. The intensity-time data were converted by the contractor to concentration-depth data by the use of intensity yield factors obtained from substitute standards and from measured rates of penetration.

The substitute standards used were stainless steel of known composition which provided approximate yield factors for carbon, chromium, iron, nickel, and molybdenum; Al_2O_3 and Si_3N_4 which provided factors for nitrogen and oxygen; and the pure elements which provided factors for aluminum, titanium, vanadium, and cobalt. A yield factor for fluorine was assumed to be approximately the same as that of chlorine or of oxygen.

Precise quantitative values would require a calibration and standard for each matrix penetrated (oxide, intermetallic, or superalloy) but these were not available nor practical for the purpose of this exploratory analysis. In this analysis, the lack of precise yield factors was assumed by the contractor to affect only the position, not the shape, of the concentration-depth gradients.

Corrections were not made for any Gaussian character of the erosion hole which is about 0.3 millimeter in diameter. Without this correction, the indicated concentration-depth profile for a species undergoing an abrupt change from a high to a low concentration appears more gradual. Otherwise claims for the analyses were implied (by the contractor) to be quantitative.

APPENDIX C

X-RAY DIFFRACTION CONSIDERATIONS

Table VI shows a tabulation of interplanar spacings, d, and X-ray diffraction peak intensity ratios ($I_{individual\ peak}/I_{most\ intense\ peak}$)100 which contain some of the major phases found in an aluminide coated nickel superalloy. In many cases the ASTM intensity ratios are rather crude approximations and may be reversed from one pattern to another. The data for NiAl, alpha chromium, alpha iron, and Ni_3Al (gamma prime) are from reference 10, and the spacings have been rounded off to two decimal places for ease of examination. The lattice spacings for the nickel solid solution have been calculated on the basis of a lattice parameter (a_o = 3.59 Å) commonly observed in nickel superalloys. The intensity data, however, are for pure nickel from reference 10. Note the similarity in patterns between MAl, Cr, and Fe. If the 2.87 Å and 1.66 Å lines are missing or weak in MAl, as frequently occurs, differentiation between these phases can be very difficult. Similarly, if the 3.60 Å and 2.55 Å lines of Ni_3Al are weak, again as frequently occurs, it is very difficult to differentiate Ni_3Al from nickel solid solution.

TABLE VI. - X-RAY DIFFRACTION DATA

Body centered cubic lattice						Face centered cubic lattice			
NiAl		Cr		Fe		Ni_3Al		Ni solid solution	
a_o = 2.88 Å		a_o = 2.88 Å		a_o = 2.87 Å		a_o = 3.56 Å		a_o = 3.59 Å	
d, Å	I/I	d, Å	I/I	d, Å	I/I	d, Å	I/I	d, Å	I/I
2.87	[a]40	----	---	----	---	3.60	[a]40	----	---
2.02	100	2.04	100	2.02	100	2.55	[a]40	----	---
1.66	[a]20	----	---	----	---	2.07	100	2.07	100
1.43	20	1.44	16	1.43	20	1.80	70	1.80	42
[a]1.29	10	----	---	----	---	[a]1.60	40	----	---
1.17	70	1.18	30	1.17	30	[a]1.46	20	----	---
1.02	20	1.02	18	1.01	10	1.27	60	1.27	21
----	---	.91	20	.90	12	1.08	60	1.08	20
----	---	.84	6	.83	6	1.03	40	1.04	7
						.89	20	.90	4
						.82	70	.82	14
						.80	70	.80	15

[a]Frequently much lower and in some cases not detected.

It must be remembered that each of the previous phases can exist over a range of compositions. Also, various atoms can substitute for nickel or aluminum in some of these compounds. For example, the composition of gamma prime in IN-100 was determined by chemical extraction to be $Ni_{2.49}Co_{0.39}(Al_{0.56}Ti_{0.34}V_{0.05}Mo_{0.03})$ rather than simply Ni_3Al (ref. 13). Such variations in composition can also cause the lattice spacings of a phase to vary. Furthermore, when a number of phases are present in a mixture, as is the case in an aluminide coating, the intensities of all peaks are depressed. In many cases, the intensities of the weaker peaks drop into the background range and cannot be detected. Finally, preferred orientation effects can increase or decrease the intensity of particular diffraction peaks.

REFERENCES

1. Goward, G. W.; Boone, D. H.; and Giggins, C. S.: Formation and Degradation Mechanisms of Aluminide Coatings on Nickel-Base Superalloys. Trans. ASM, vol. 60, no. 2, June 1967, pp. 228-241.

2. Fornwalt, D. E.; and Boone, D. H.: Metallographic Characterization of Phases Associated with Aluminide Coated Udimet 700. Proceedings of the 1st Annual Technical Meeting International Metallographic Society. K. A. Johnson and J. H. Bender, eds., International Metallographic Society, 1969, pp. 97-111.

3. Moore, V. S.; Brentnall, W. D.; and Stetson, A. R.: Evaluation of Coatings for Cobalt and Nickel-Base Superalloys. Vol. 1. Rep. RDR-1474-2, Solar (NASA CR-72359), Jan. 31, 1969.

4. Felten, Edward J.: High-Temperature Oxidation of Fe-Cr Base Alloys with Particular Reference to Fe-Cr -Y Alloys. J. Electrochem. Soc., vol. 108, no. 6, June 1961, pp. 490-495.

5. Barrington, A. E.; Herzog, R. F. K.; and Poschenreider, W. P.: The Ion Microprobe Mass Spectrometer. Analytical Chemistry. Series IX, vol. 7 of Progress in Nuclear Energy. H. A. Elion and D. C. Stewart, eds., Pergamon Press, 1966, pp. 243-273.

6. Herzog, R. F. K.; Poschenreider, W. P.; and Satkiewicz, F. G.: Mass Spectrometer Analysis of Solid Materials with the Ion-Microprobe Sputter Source. NASA CR-683, 1967.

7. Liebl, Helmut: Ion Microprobe Mass Analyzer. J. Appl. Phys., vol. 38, no. 13, Dec. 1967, pp. 5277-5283.

8. Rouberol, J. M.; Guernet, J.; Deschamps, P.; Dagnot, J. P.; and Guyon de la Berge, J. M.: Secondary Ion Emission Microanalyzer. Presented at the 16th Annual Conference on Mass Spectrometry and Allied Topics, Pittsburgh, Pa., May 12-17, 1968.

9. Robinson, C. F.; Andersen, C. A.; and Roden, H. J.: Progress in the use of the Ion Microprobe for the Isotopic Microanalysis of Solids. Presented at the 20th Pittsburgh Conference on Analytical Chemistry and Applied Spectroscopy, Cleveland, Ohio, Mar. 2-7, 1969.

10. Anon.: 16th Set of Inorganic Powder Diffraction File. ASTM, 1966.

11. Sabol, G. P.; and Stickler, R.: Microstructure of Nickel-Based Superalloys. Phys. Stat. Sol., vol. 35, no. 1, 1969, pp. 11-52.

12. Restall, J. E.: An Examination of Correction Procedures for Quantitative Electron-Probe Microanalysis. Metallurgia, vol. 80, no. 479, Sept. 1969, pp. 121-125.

13. Kriege, Owen H.; and Baris, J. M.: The Chemical Partitioning of Elements in Gamma Prime Separated for Precipitation-Hardened, High-Temperature Nickel-Base Alloys. Trans. ASM, vol. 62, no. 1, Mar. 1969, pp. 195-200.

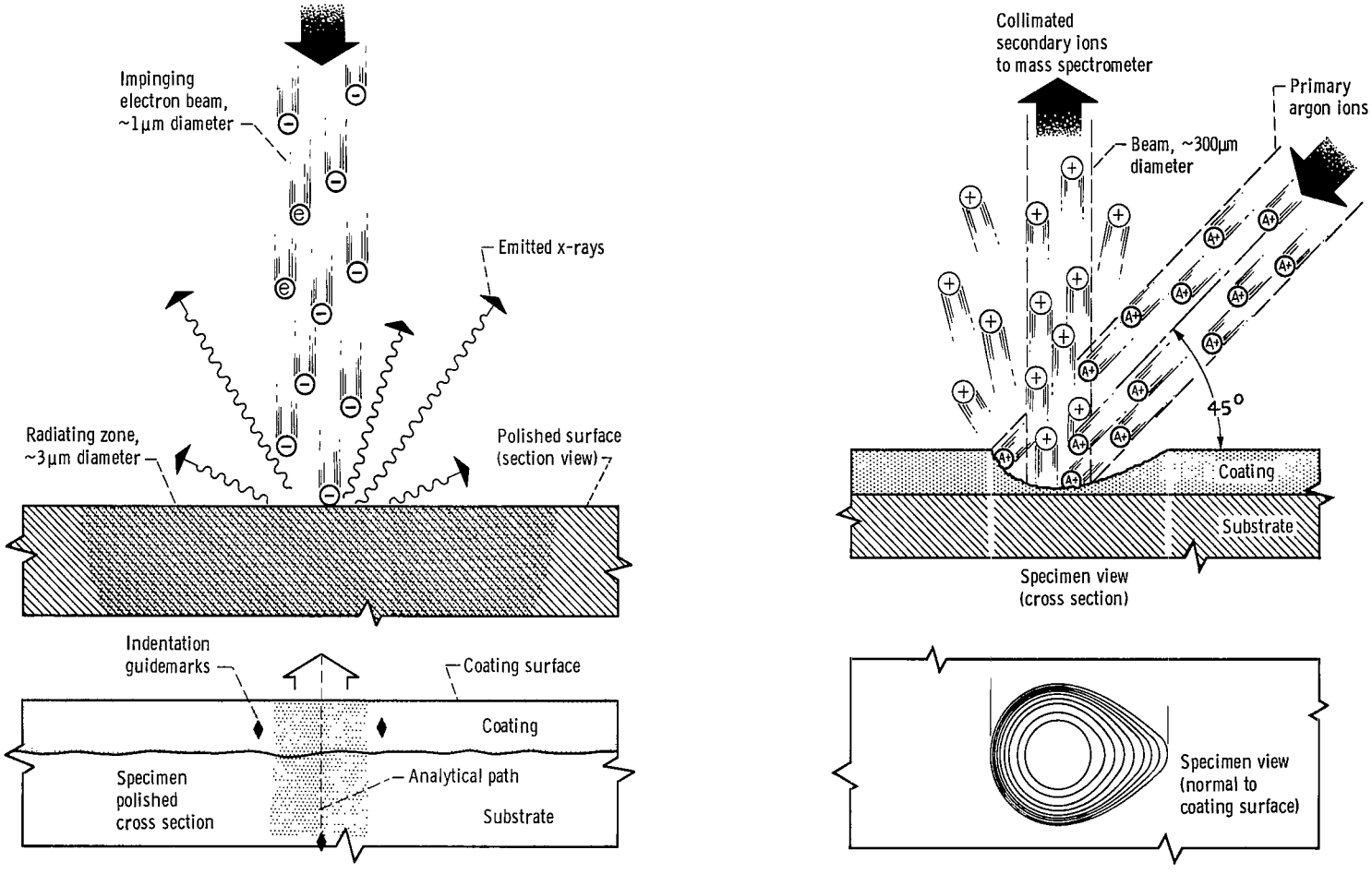

(a) Electron microprobe (EMP) analyzer.

(b) Ion beam mass spectrometer probe analyzer.

Figure 1. - Representation of specimen undergoing microprobe analysis.

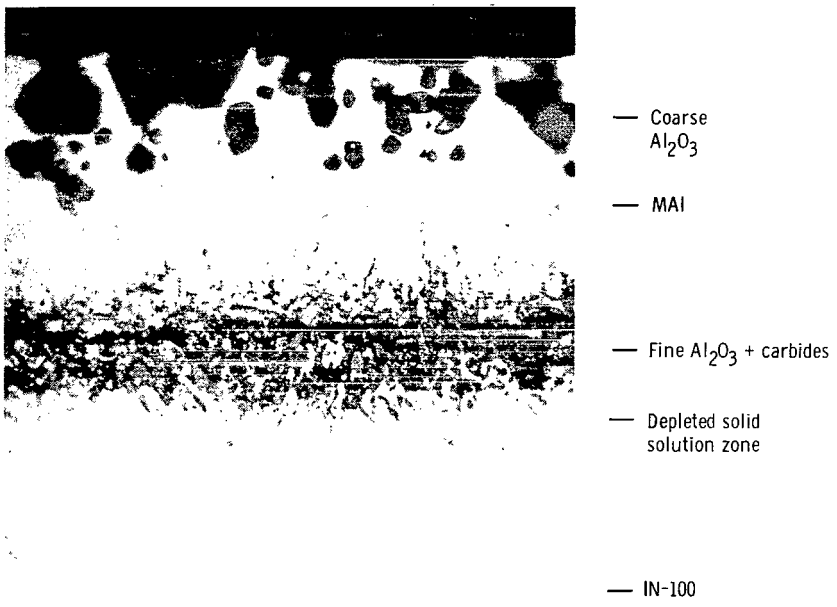

(a) As-coated.

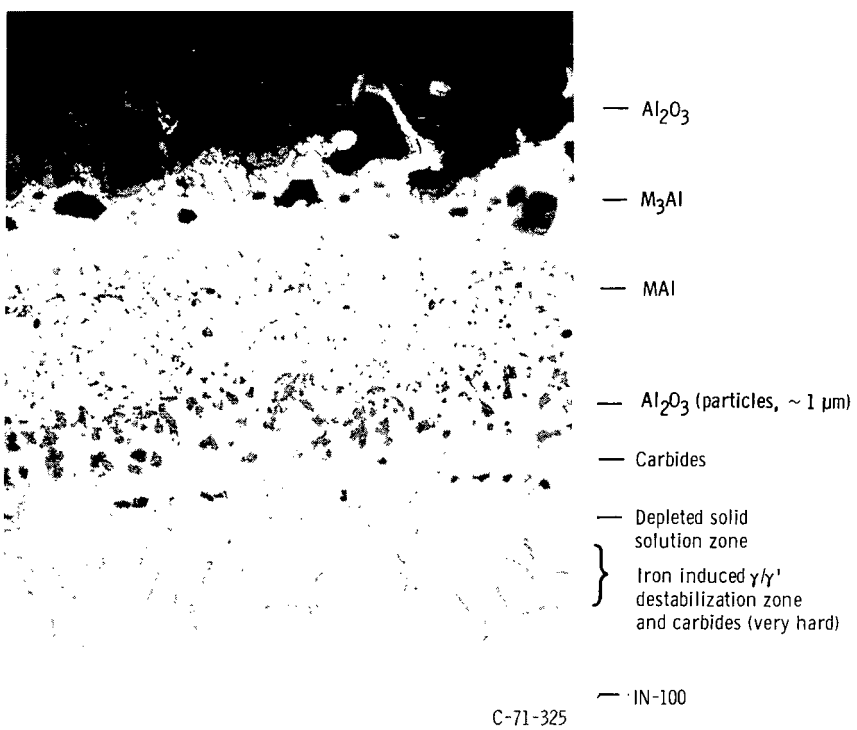

(b) As-oxidized.

Figure 2. - Unetched cross sections of an experimental aluminide coating on IN-100. X400.

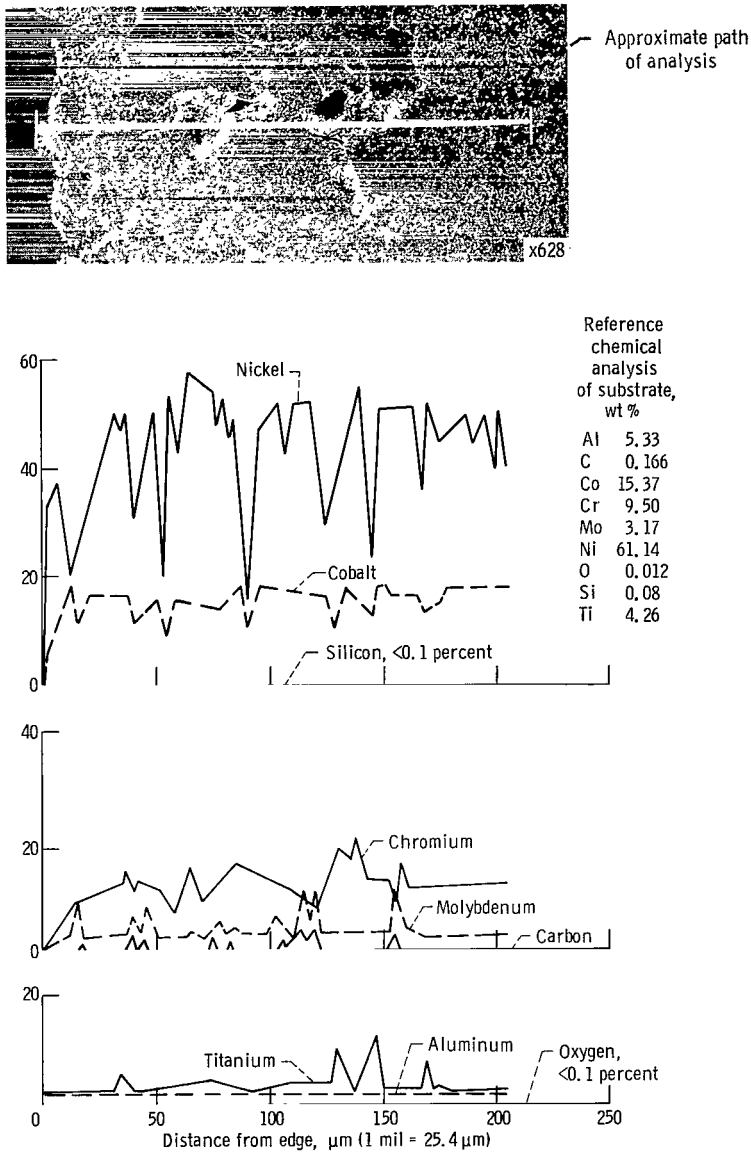

Figure 3. - Substrate superalloy IN-100 in as-received uncoated condition. Analyzed by electron microprobe (specimen 5406). Micrograph etched after analysis.

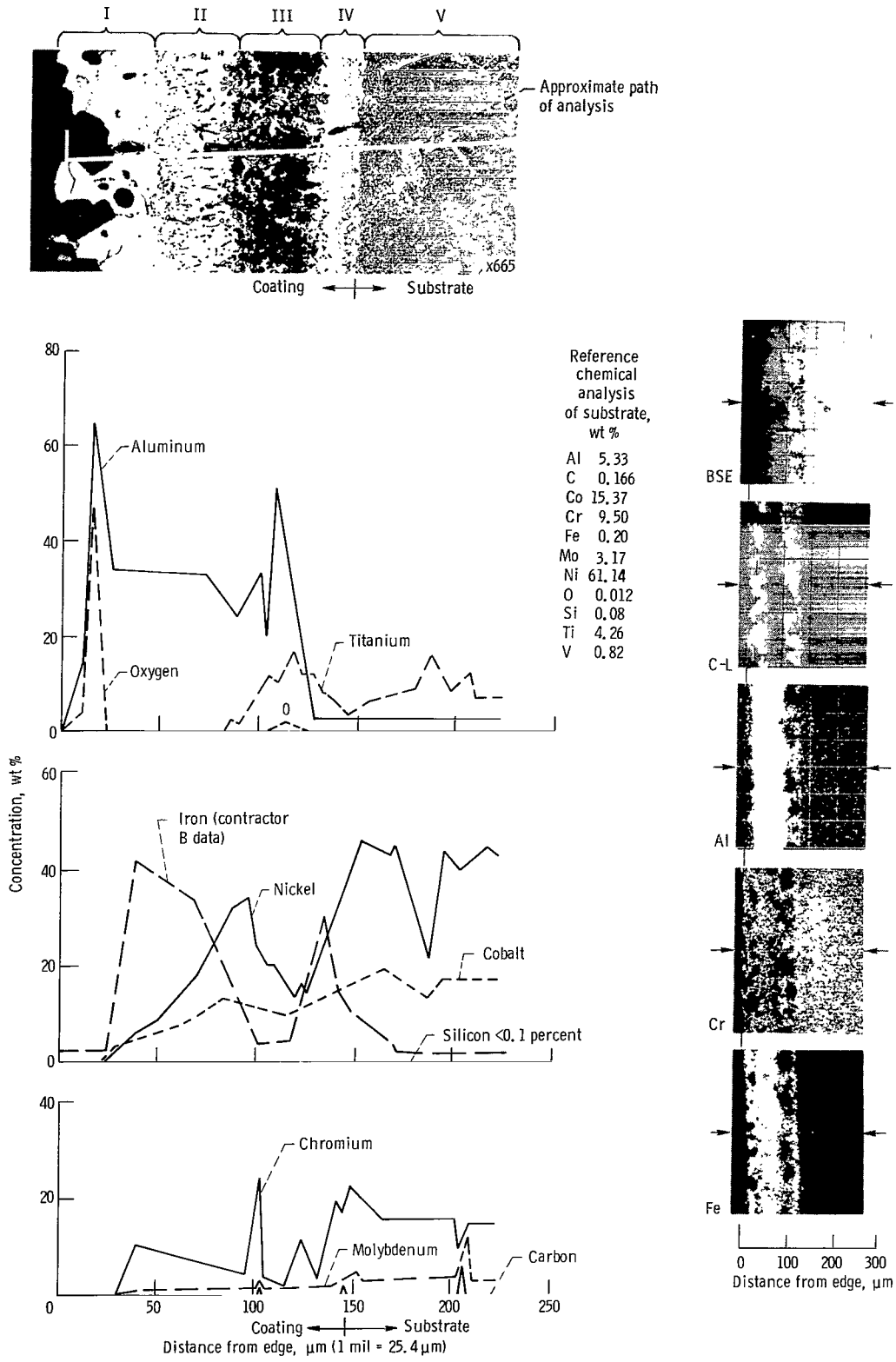

Figure 4. - Superalloy IN-100 as-coated with aluminide. Analyzed by electron microprobe (specimen 5403). Micrograph etched after analysis. Arrows on scanning micrograph denote analytical path.

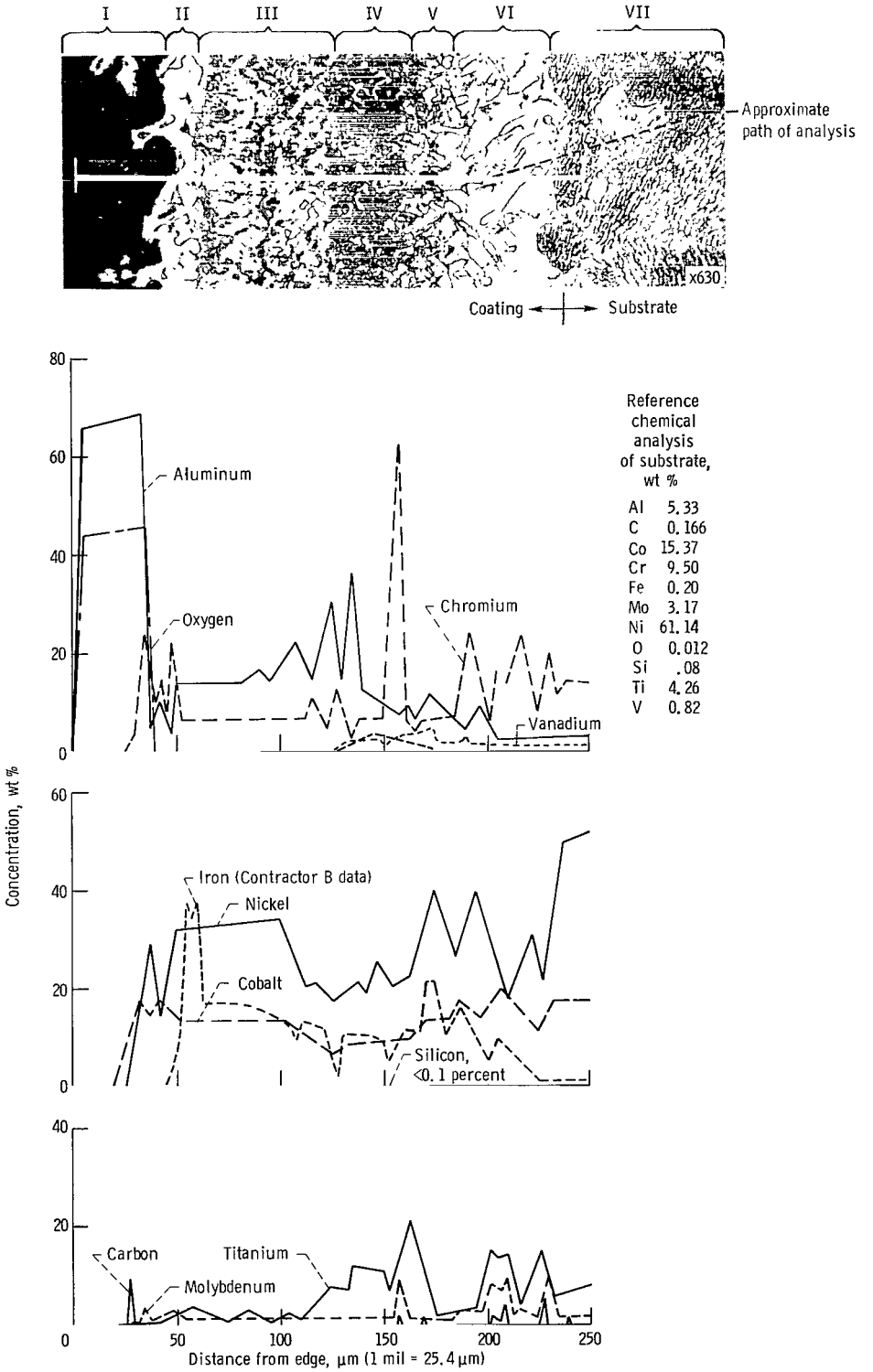

Figure 5. - Superalloy IN-100 coated with aluminide and after oxidation at 1900° F (1038° C) for 100 hours in air. Analyzed by electron microprobe (specimen 5405). Micrograph etched after analysis.

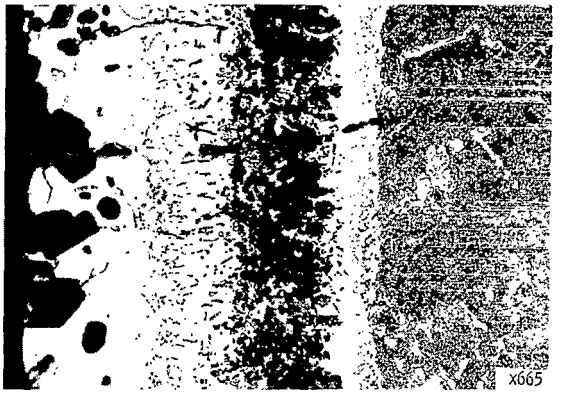

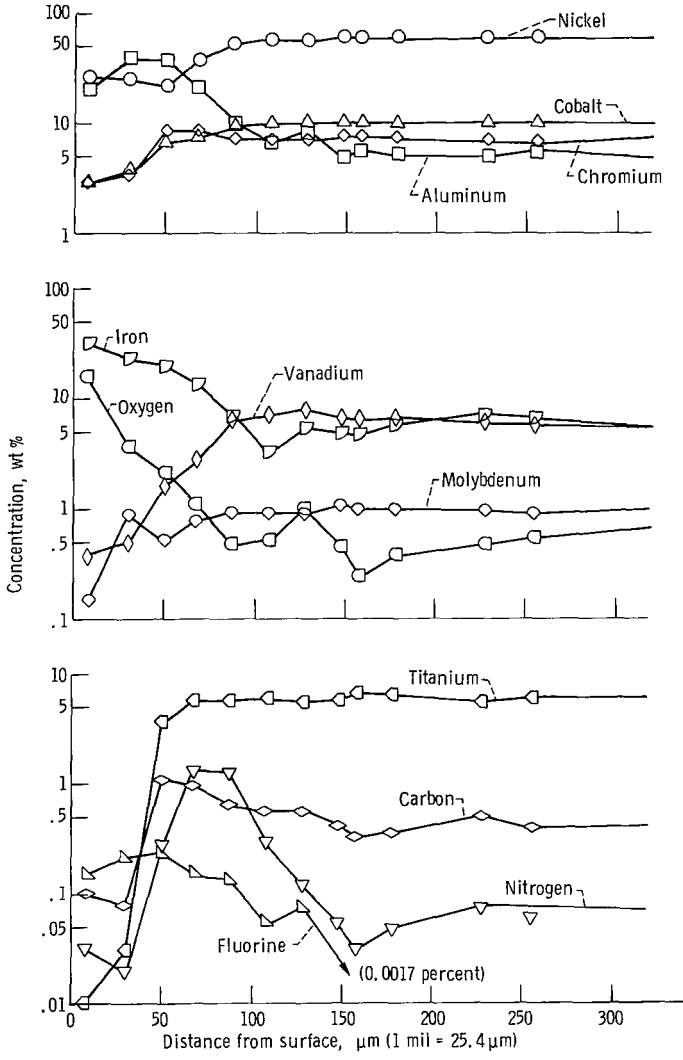

Spectro-chemical analysis of substrate, wt %

Al	5.33
C	0.166
Co	15.37
Cr	9.50
Fe	0.20
Mo	3.17
N	0.006
Ni	61.14
O	0.012
Si	0.08
Ti	4.26
V	0.80

Figure 6. - Analysis by ion beam mass spectrometer. Specimen was superalloy IN-100 as-coated with aluminide. Micrograph etched after analysis.

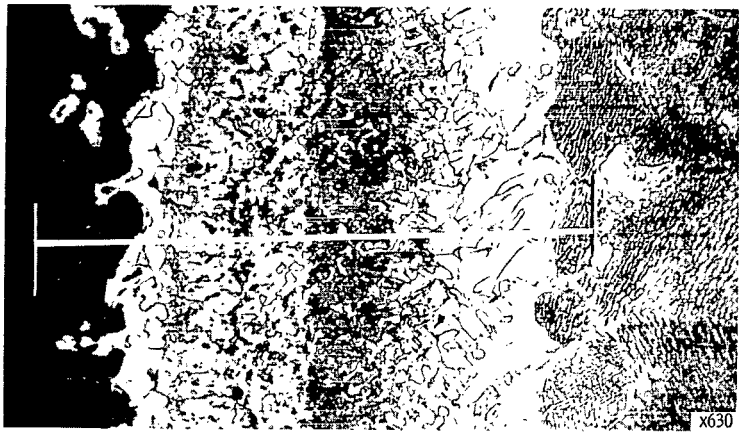

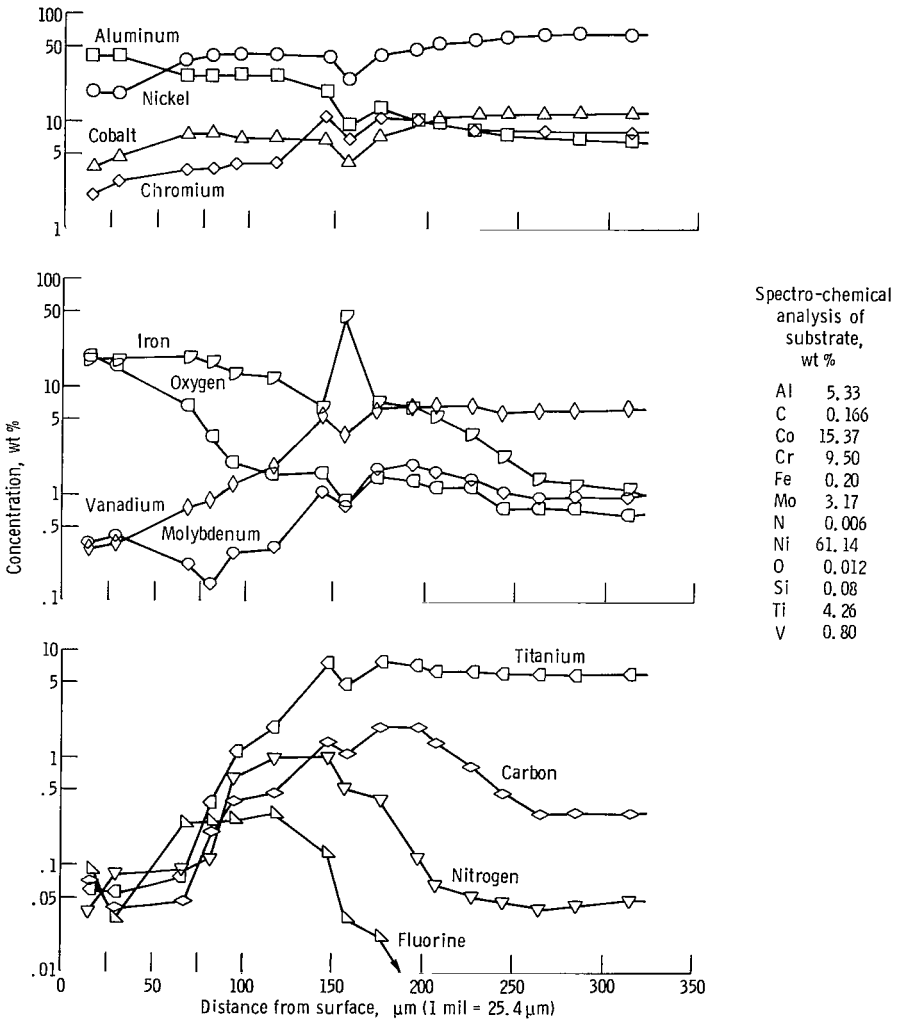

Spectro-chemical analysis of substrate, wt %

Al	5.33
C	0.166
Co	15.37
Cr	9.50
Fe	0.20
Mo	3.17
N	0.006
Ni	61.14
O	0.012
Si	0.08
Ti	4.26
V	0.80

Figure 7. - Analyses by ion beam mass spectrometer specimen was superalloy IN-100 coated with aluminide. Condition was after oxidation at 1900° F (1038° C) in air for 100 hours. Micrograph etched after analysis.

06U 001 42 51 3DS 71135 00903
AIR FORCE WEAPONS LABORATORY /WLOL/
KIRTLAND AFB, NEW MEXICO 87117

ATT E. LOU BOWMAN, CHIEF,TECH. LIBRARY

"The aeronautical and space activities of the United States shall be conducted so as to contribute . . . to the expansion of human knowledge of phenomena in the atmosphere and space. The Administration shall provide for the widest practicable and appropriate dissemination of information concerning its activities and the results thereof."

—NATIONAL AERONAUTICS AND SPACE ACT OF 1958

NASA SCIENTIFIC AND TECHNICAL PUBLICATIONS

TECHNICAL REPORTS: Scientific and technical information considered important, complete, and a lasting contribution to existing knowledge.

TECHNICAL NOTES: Information less broad in scope but nevertheless of importance as a contribution to existing knowledge.

TECHNICAL MEMORANDUMS: Information receiving limited distribution because of preliminary data, security classification, or other reasons.

CONTRACTOR REPORTS: Scientific and technical information generated under a NASA contract or grant and considered an important contribution to existing knowledge.

TECHNICAL TRANSLATIONS: Information published in a foreign language considered to merit NASA distribution in English.

SPECIAL PUBLICATIONS: Information derived from or of value to NASA activities. Publications include conference proceedings, monographs, data compilations, handbooks, sourcebooks, and special bibliographies.

TECHNOLOGY UTILIZATION PUBLICATIONS: Information on technology used by NASA that may be of particular interest in commercial and other non-aerospace applications. Publications include Tech Briefs, Technology Utilization Reports and Technology Surveys.

Details on the availability of these publications may be obtained from:

SCIENTIFIC AND TECHNICAL INFORMATION OFFICE

NATIONAL AERONAUTICS AND SPACE ADMINISTRATION

Washington, D.C. 20546